13

Computer Modeling of Heterojunction with Intrinsic Thin Layer "HIT" Solar Cells: Sensitivity Issues and Insights Gained

Antara Datta and Parsathi Chatterjee
Energy Research Unit, Indian Association for the Cultivation of Science, Jadavpur, Kolkata, India

1. Introduction

Despite significant progress in research, the energy provided by photovoltaic cells is still a small fraction of the world energy needs. This fraction could be considerably increased by lowering solar cell costs. To achieve this aim, we need to economize on the material and thermal budgets, as well as increase cell efficiency. The silicon "**H**eterojunction with **I**ntrinsic **T**hin layer (HIT)" solar cell is one of the promising options for a cost effective, high efficiency photovoltaic system. This is because in "HIT" cells the P/N junction and the back surface field (BSF) layer formation steps take place at a relatively low temperature (~200°C) using hydrogenated amorphous silicon (a-Si:H) deposition technology, whereas in normal crystalline silicon (c-Si) cells the wafer has to be raised to ~800°C for junction and BSF layer formation by diffusion. This means not only a lower thermal budget, but also cost reduction from thinner wafers, since the danger of the latter becoming brittle is strongly reduced at lower (~200°C) temperatures. Thin intrinsic layers on either face of the c-Si substrate, effectively passivate c-Si surface defects, which would otherwise degrade cell performance. Moreover it has been demonstrated that carriers can pass through the passivating layers without significant loss.

In this chapter, we use detailed electrical-optical modeling to understand carrier transport in these structures and the sensitivity of the solar cell output to various material and device parameters. The global electrical - optical model "Amorphous Semiconductor Device Modeling Program (ASDMP)", originally conceived to simulate the characteristics of solar cells based on disordered thin films, and later extended to model also mono-crystalline silicon and "HIT" solar cells (Nath et al, 2008), has been used for all simulations in this chapter. The model takes account of specular interference effects, when polished c-Si wafers are used, as well as of light-trapping when HIT cells are depositd on textured c-Si.

2. Historical development of HIT solar cells

One of the successful applications of hydrogenated amorphous silicon (a-Si:H) is in crystalline silicon heterojunction (HJ) solar cells. Fuhs et al (1974) first fabricated heterojunction silicon solar cells, where the absorber is P (N) type c-Si, while the emitter N

(P) a-Si:H layer is deposited by the standard plasma-enhanced chemical vapor deposition (PECVD) technique at ~200°C. However the efficiency achieved was much lower than in c-Si solar cells. In the early 80's Prof. Y. Hamakawa and his co-workers [Osuda et al, 1983] predicted the relevance of a-Si:H /c-Si stacked solar cells in silicon applications. Following the study of Prof. Hamakawa, many research groups world wide became interested in the technological development of a-Si:H/c-Si heterojuction solar cells as an alternative to traditional diffused emitter solar cells. It was almost a decade later that Sanyo began work in 1990 on the growth of low temperature junctions on c-Si and developed a new type of heterojunction solar cells called ACJ-HIT (Artificially Constructed Junction- Heterojunction with Intrinsic Thin layer), now shortened to "HIT", with a conversion efficiency of 18.1% (Tanaka et al, 1992) that has thereafter been continuously improved to yield an outstanding 22% efficiency in 100 cm² solar cells (Taguchi et al, 2005). Moreover Sanyo also achieved 19.5% efficiency in mass production (Tanaka et al, 2003). The innovation that made this possible was the introduction of thin films of intrinsic a-Si:H on either side of the c-Si wafer, to passivate the defects on its surface, that were responsible for the low efficiency of the earlier heterojunction cells [Fuhs et al, 1974]. A low recombination surface velocity of 15 cm/s has been demonstrated for passivation by intrinsic a-Si:H by Wang et al (2005). This is as good as the best dielectric surface passivation, such as by SiO_2 and amorphous silicon nitride (SiN_x) (Meier et al, 2007). More importantly, the a-Si:H I-layer can be inserted between the c-Si and a doped layer without significant restriction to carrier transport. The device structure of HIT cells that has been developed by Sanyo is shown in Fig. 1. This cell is fabricated with CZ N-type wafer of thickness ~250 μm. The emitter (doped) layer, passivating intrinsic layers and the doped BSF layer of the cell are all thin films (a-Si:H) and deposited by the PECVD technique at ~200°C. The device terminates with a TCO anti reflection coating followed by metallic electrodes.

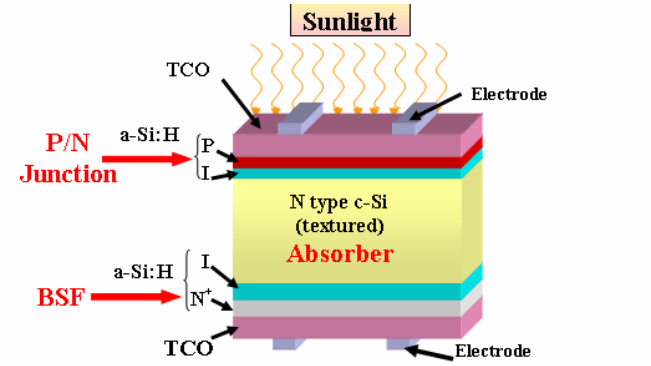

Fig. 1. Schematic diagram of HIT cell proposed by SANYO

HIT cells have (1) potential for high efficiency, (2) very good surface passivation: low surface recombination velocity, (3) low processing temperature - all processes occur at ~ 200°C resulting in low thermal budget, (4) reduced material cost (low temperature processing permits the use of thinner wafers), leading to overall cost reduction and (5) excellent stability- since the base material of the structure continues to be c-Si. With nearly 19 years of steady progress, in 2009, the best HIT solar cells have recorded a efficiency of 23% over a 100.4 cm² cell area (press release SANYO, 2009). Another advantage of HIT solar

cells is that it has excellent temperature dependence characteristics and its efficiency does not deteriorate as much as that of diffused junction c-Si cells at higher temperatures (Sakata et al, 2000). The efficiency of HIT cells deteriorates by 0.33%/° C with increase of temperature while it is 0.45%/° C for conventional c-Si solar cells. This means HIT cells would generate more output power in summer time than its diffused junction counterpart.

References	Wafer		Solar cell output parameters				Emitter & BSF deposition technique
	Type	Surface	J_{sc} mA cm^{-2}	V_{oc} mV	Fill factor	η %	
SANYO press release	N	Textured	39.50	729	0.800	23	PECVD
Schmidt et al, 2007	N	Textured	39.3	639	0.789	19.8	RF-PECVD
	P		34.3	629	0.79	17.4	
Wang et al, 2010,2008	P	Textured	36.20	678	0.786	19.3	HWCVD
	N		35.30	664	0.745	17.2	
Olibet et al, 2010, 2007	N	Flat	34.0	680	0.82	19.1	VHF-PECVD
	P		32	690	0.74	16.3	
Das et al, 2008	N	Textured	35.68	694	0.741	18.4	PECVD
Sritharathikhun et al 2008	N	Textured	35.20	671	0.76	17.9	VHF-PECVD
Damon-Lacoste, 2008	P	Flat	33.0	664	0.778	17.1	PECVD
Fujiwara & Kondo, 2009	N	Flat	32.79	631	0.764	17.5	PECVD

Table 1. Summary of best perfoemances of HIT solar cells on P- and N-type c-Si wafer.

Inspired by the outstanding performance of Sanyo HIT cells, many research groups throughout the world have been working with these cells and a-Si:H layers have been deposited by PECVD, hot-wire CVD (HWCVD) and very-high-frequency PECVD (VHF-PECVD). A summary of the best HIT solar cells reported till date is given in Table 1. We find that currently, no group has been able to duplicate what Sanyo has achieved in terms of cell efficiency. Very few groups have reached beyond 19% efficiency: Helmholtz Zentrum Berlin on N-type textured wafers (Schimdt et al, 2007) and the National Renewable Energy Laboratory (NREL) on P-type textured wafers (Wang et al, 2008, 2010) have achieved this feat. Good results have also been obtained by the group of EPFL, IMT, Neuchâtel, Switzrland with high open-circuit voltsge (V_{oc}) on flat wafers. The P-type HIT cell of Damon Lacoste et al (2008) from LPICM-Ecole Polytechnique, France also deserves mention. Here the efficiency is limited by the lower short-circuit current density (J_{sc}) characteristic of flat wafers. The difficulty in attaining the Sanyo HIT cell efficiency illustrates that the a-Si:H/c-Si HJ is indeed a very challenging structure to understand. Therefore, over the last decade scientists are using detailed computer modeling to fully understand the structure. In the next section we will briefly review the computer modeling of HIT solar cells. Recently a few groups have started fabricating HIT cells with intrinsic hydrogenated amorphous silicon oxide (I-a-SiO:H) as the buffer layer between crystalline and doped amorphous silicon. Sritharathikhun et al (2008) have achieved 17.9% cell efficiency with P-μc-SiO:H /N-c-Si cell structure and I-a-SiO:H as the buffer layer. A group from AIST (Fujiwara et al, 2009) has reported 17.5% cell efficiency with a similar cell structure.

2.1 Detailed one-dimensional computer modeling of HIT solar cells:-

Pioneering work in detailed electrical modeling of a-Si:H solar cells was done by Hack and Schur (1985). Other notable models in this respect are the model AMPS (McElheny et al, 1988, Arch et al, 1991) by S. J. Fonash's group at the Pennsylvania State University, USA, the model of Guha's group (Guha et al, 1989), the ASDMP program by P. Chatterjee (Chatterjee, 1992, 1994, 1996), the ASPIN program of Smole and Furlan (1992) and the ASA program by von der Linden et al (1992). Regarding detailed electrical-optical models, which include textured surfaces and light-trapping kinetics to some extent, the first global electrical-optical model developed in the world was when ASDMP was integrated (Chatterjee et al, 1996) to a semi-empirical optical model by Leblanc et al (1994). This program also takes account of specular interference effects for cells with flat surfaces. Later the developed AMPS program (D-AMPS – Plà et al, 2003) and the ASA package, developed at the Delft University of Technology (Zeman et al, 2000) also introduced light trapping effects.

Modeling of HIT cells was started by van Cleef et al (1998 a,b) using the AMPS computer code (McElheny et al, 1988), which however does not have a proper built-in optical model; and the derivative of the AMPS program (D-AMPS), where a fairly good optical model has been introduced (Plà et al, 2003). The numerical PC program AFORS-HET (Stangl et al, 2001, Froitzheim et al, 2002) has been developed especially for simulating HIT solar cells. The latter has recently also been extended to include light-trapping effects. The ASA program in its later version (Zeman et al, 2000) models both the electrical and optical properties of HIT cells. The PC-1D program (Basore, 1990, Basore et al, 1997), developed at the University of News South Wales, Australia for modeling textured mono-crystalline silicon solar cells, has also been fairly successful in modeling HIT cells. The program ASDMP by Chatterjee et al (1994,1996), has also been extended to model N-a-Si:H/P-c-Si type front (with a heterojunction only on the emitter side) (Nath et al, 2008) HIT cells and subsequently used to model double hetreojunction solar cells both on N- and P-type substrates (Datta et al, 2008, 2009, Rahmouni et al, 2010).

2.1.1 Simulation model ASDMP

We will discuss this model in a little more detail, since it has been used in all simulations in this chapter. The "Amorphous Semiconductor Device Modeling Program (ASDMP) " (Chatterjee et al, 1996, Palit et al, 1998), originally conceived to model amorphous silicon based devices, has been extended to also model c-Si and "HIT" cells (Nath et al, 2008). This one-dimensional program solves the Poisson's equation and the two carrier continuity equations under steady state conditions for the given device structure, without any simplifying assumptions, and yields the dark and illuminated current density - voltage (J-V), the quantum efficiency (QE) and the photo- and electro-luminescence characteristics of HIT cells. Its electrical part is described in P. Chatterjee (1994, 1996). The gap state model used in these calculations for the amorphous layers, consists of the tail states and the two Gaussian distribution functions to simulate the deep dangling bond states, while in the c-Si part, the tail states absent. The lifetime of the minority carriers inside the N(P) -c-Si wafer may be estimated using the formula:

$$\tau_p \approx \frac{p - p_0}{R} \quad \text{or} \quad \tau_n \approx \frac{n - n_0}{R}, \tag{1}$$

where $\tau_p(\tau_n)$, $p(n)$ and $p_0(n_0)$ are the minority carrier lifetime, its density under the given experimental conditions (in this case under 100 mW cm^{-2} of AM1.5 light), and at thermodynamic equilibrium respectively; while R is the recombination rate in the c-Si wafer. The lifetime, calculated in this manner, is in general, position-dependent; however over a large region inside the c-Si wafer, away from the edges, it is a constant and it is this value that is taken to be the minority carrier lifetime in the wafer. van Cleef et al (1998a,b) and Kanevce et al (2009) have also used the DOS model to simulate their HIT cells.

The generation term in the continuity equations has been calculated using a semi-empirical model (F. Leblanc et al, 1994) that has been integrated into the ASDMP modeling program (Chatterjee et al, 1996, Palit et al, 1998). Both specular interference effects and diffused reflectance and transmittance due to interface roughness can be taken into account. The complex refractive indices for each layer of the structure, required as input to the modeling program, have been measured by spectroscopic ellipsometry. In all cases studied in this article, experimentally or by modeling, light enters through the transparent conducting oxide (TCO)/emitter window, which is taken as x = 0 on the position and referred to as the front contact. Voltage is also applied at x = 0. The BSF/ metal contact at the back of the c-Si wafer is taken as x = L on the position scale, where L is the total thickness of all the semiconductor layers of the device. This back contact is assumed to be at ground potential.

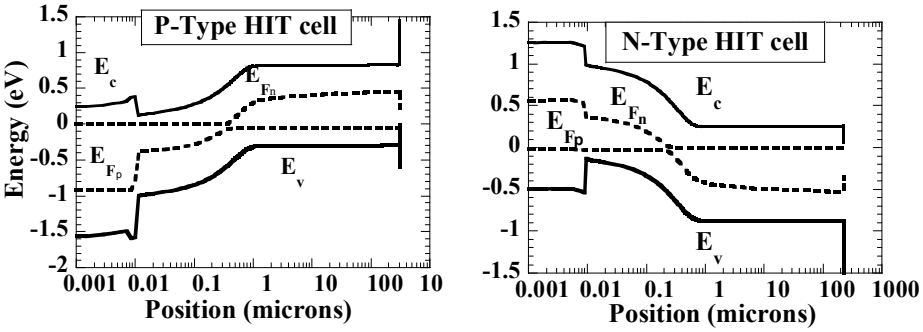

Fig. 2. Energy band diagram for HIT solar cells on P and N type wafers under 100 mW of AM1.5 light and short-circuit conditions.

The calculated energy band diagrams for typical HIT cells on P- and N-type wafers, with passivated surface defects and under 100 mW of AM1.5 light, 0 volts, are shown in Fig. 2.

4. Modeling of HIT solar cells on P-type wafer

4.1 Simulation of experimental results of P-type HIT cells

We have studied both front and double "HIT" structure solar cells on P-type c-Si wafers. These have the structure: N-a-Si:H emitter/ P-c-Si/ aluminum diffused BSF (front HIT) and N-a-Si:H emitter/ P-c-Si/ P$^+$-a-Si:H BSF (double HIT). The experimental data were obtained from the Laboratoire de Physique des Interfaces et des Couches Minces (LPICM), Ecole Polytechnique, Palaiseau, France. Table 2 compares our modeling results to the measured output parameters for front and double HIT structures. Two thicknesses of the N-a-Si:H layer are employed for the front HIT structures, while results are given for two types of

double HIT cells having the following structures: (A) 8 nm N-a-Si:H/ 3 nm pm-Si:H intrinsic layer/ P-c-Si wafer/ 23 nm P^+-a-Si:H/ 1.5 μm Al, and (B) the above structure, but with a 4 nm P^+-a-SiC:H layer sandwiched between the P-c-Si wafer and a 19 nm P^+-a-Si:H layer. The pm-Si:H intrinsic layer on the front surface (FS) of the c-Si wafer is there to passivate the defects on this surface. However, no such passivating layer has been deposited on the rear surface (RS) of the c-Si wafer. The defect density on FS was deduced by modeling to be 10^{11} cm^{-2}. Cell B, which has a 4 nm P-type a-SiC:H layer on the rear c-Si wafer surface, has a slightly higher V_{oc} but a lower FF relative to case A, leading to a better efficiency. However, we could not replicate these results in our modeling calculations by the introduction of a P^+-a-SiC:H layer of the given properties alone (case B1 in Table 2). In fact, the defect density on the rear wafer surface had to be slightly reduced (case B2, Table 2) to match the experimental results.

Table 2 indicates good agreement between experiments and modeling, except that our modeling results appear to overestimate the FF and hence the efficiency of front HIT cells. In reality this is because screen-printed contacts with low temperature silver paint was used for these cells; resulting in high series resistance and low FF experimentally, which cannot be accounted for by modeling. For double HIT structures, developed later, improved contact formation resulted in very low series resistance and high fill factors experimentally, which agree well with model calculations (Table 2).

HIT type	Sample	N-a-Si:H (nm)	N_{ss} on the DL (cm^{-2})	V_{oc} (mV)	J_{sc} (mA cm^{-2})	FF	η(%)
Front	X1 (E)	12		634	31.90	0.711	14.38
	X1 (M)	12	FS- $4x10^{11}$	636	31.85	0.823	16.67
	X2 (E)	8		640	32.54	0.730	15.20
	X2 (M)	8	FS- $4x10^{11}$	640	32.57	0.824	17.18
Double	A (E)	8		650	32.90	0.790	16.90
	A (M)	8	FS-10^{11} RS-$8x10^{11}$	660	32.84	0.781	16.93
	B (E)	8		664	33.10	0.779	17.12
	B1(M)		FS-10^{11} RS-$8x10^{11}$	653	33.17	0.749	16.24
	B2 (M)	8	FS-10^{11} RS- $3x10^{11}$	667	33.21	0.773	17.12

Table 2. Comparison between measured (E) and modeled (M) solar cell output parameters of front and double P-c-Si HIT cells with a flat ITO front contact. DL refers to the defective layer on the wafer surface.

In Fig. 3 (a), we compare the experimentally measured external and internal quantum efficiency (EQE and IQE respectively) curves of the solar cell B to modeling results, while in Fig. 3 (b) we compare the measured IQE curves of a front HIT and the above-mentioned double HIT solar cells, both deposited in the same reactor and under approximately the same conditions of RF power and pressure as solar cells A and B above. The IQE is obtained from the EQE using the formula:

$$IQE(\lambda) = EQE(\lambda) / (1 - R(\lambda) - ITOabs(\lambda)) , \quad (2)$$

where $R(\lambda)$ is the reflectivity of the HIT cell and $ITOabs(\lambda)$ is the fraction of the light that is absorbed in the transparent conducting oxide, that is indium tin oxide (ITO) in this case.

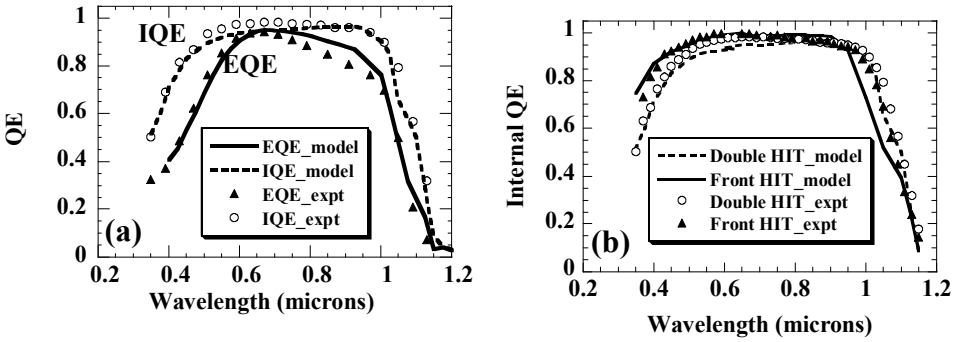

Fig. 3. Comparison of the experimentally measured external and internal QE curves of (a) a double heterojunction cell (case B2 of Table 2); and (b) of a front and the above double HIT solar cell, to modeling results, indicating a higher long wavelength IQE for the double HIT case, both experimentally and in the modeling calculations. The ITO layer is different for the two cases resulting in the difference in the short wave length QE. The lines represent the calculated results, experimental measurements are shown as symbols.

We have used the above simulations to extract the parameters that characterize different layers of the double HIT cells A and B on P-type wafers. These are given in Table 3, together with the extracted parameters of double HIT cells on N-type wafers. The experimental results used to extract the latter and comments thereon, will be discussed in section 5.1. The data in Table 3 includes some measured data: the thickness and doping density of each layer/ wafer, the band gaps of the layers and the electron and hole mobility in the c-Si wafer (Sze, 1981). We also found that a higher value of N_{ss} (as indicated in Case B2 in Table 2 and Table 3) was necessary at the RS to simulate the experimental results. No layer was intentionally deposited to passivate these defects in cells A and B.

Since the 4-nm P^+-a-SiC:H layer on the RS of the c-Si wafer (part of the highly doped thin film BSF layer) produces a small but reproducible improvement in the overall device performance, we have tried to understand the basic reasons for this improvement. To realize the role of the thin P-a-SiC:H layer on the RS in case B2 we have made the P^+-a-SiC:H layer thicker than in case B2 and adjusted the thickness of following P^+-a-Si:H layer to yield a total BSF thickness of 23 nm. We found an all-round deterioration of the solar cell output for the thicker P^+-a-SiC:H layers, including a striking fall in the fill factor. We have thus concluded that the introduction of the thin carbide layer as such is not responsible for the observed improvement in cell efficiency of case B2 relative to case A (Table 2). Rather, it appears likely that this wider band gap material helps in passivating the defects on the RS of the c-Si wafer (for which a very thin layer is sufficient) and thereby improves cell performance. In the next section we will discuss how solar cell performance is affected by the defects on the FS and RS of the c-Si wafer.

Parameters	*N-a-Si:H/P-a-Si:H* emitter	I-pm Si:H buffer	I-a-Si:H buffer	DL on P-c-Si/ N-c-Si on emitter side	P-c-Si/N-c-si wafer	P^+-a-Si :H / N^+-a-Si : H BSF
Layer thickness (μm)	0.008/ 0.0065	0.003	0.003	0.003	300/220	0.019
Electron affinity (eV)	4	3.95	4	4.22	4.22	4
Mobility gap (eV)	1.80	1.96	1.80	1.12	1.12	1.78/1.80
Don (accep)doping (cm^{-3})	10^{19}/ $1.41x10^{19}$	0	0	$9x10^{14}$	$9x10^{14}$	$1.4x10^{19}$/ $1.45x10^{19}$
Eff. DOS in CB (cm^{-3})	$2x10^{20}$	$2x10^{20}$	$2x10^{20}$	$2.8x10^{19}$	$2.8x10^{19}$	$2x10^{20}$
Eff. DOS in VB (cm^{-3})	$2x10^{20}$	$2x10^{20}$	$2x10^{20}$	$1.04x10^{19}$	$1.04x10^{19}$	$2x10^{20}$
Exp.tail prefact. -$cm^{-3}eV^{-1}$	$4x10^{21}$	$4x10^{21}$	$4x10^{21}$	—	—	$4x10^{21}$
Charac.energy – VB tail (ED) (eV)	0.05	0.05	0.07	—	—	0.05
Charac.energy – CB tail (EA) (eV)	0.03	0.03	0.04	—	—	0.03
Elec.mobility (cm^2/V-s)	20/25	30	25	1000/1500	1000/1500	20
Hole mobility (cm^2/V-s)	6/5	12	5	450/500	450/500	6/4
Gaussian defect density (cm^{-3})	$9x10^{18}$	$7x10^{14}$	$9x10^{16}$	$2.6x10^{18}$/ $4.5x10^{18}$	10^{12}	$8x10^{18}$/ $9x10^{18}$

Table 3. Input parameters, extracted by modeling, that characterize the above HIT cells. The defect density of $3.3x10^{17}$ cm^{-3} on the front wafer surface corresponds to a defect density of 10^{11} cm^{-2} (FS) and $3.5x10^{18}$ cm^{-3} to $8x10^{11}$ cm^{-2} on the rear surface (RS). The P^+-a-SiC:H BSF layer in P-type HIT cells has a larger band gap (1.84 eV), and broader band taills: ED=0.7 eV, EA=0.5 eV

4.2 Influence of the defect density on the front surface of the c-Si wafer:

The effect on the solar cell output parameters of varying the defect density, N_{ss}, on front surface of the P-type c-Si wafer (that which faces the incoming light) is shown in Table 4, using as the base case the double HIT cell B2, but with an assumed textured wafer to reproduce state-of-the-art currents obtainable in HIT cells. The defect density on the RS is held at 10^{11} cm^{-2} for all cases. The results indicate a sharp fall in V_{oc}, and FF.

To understand the sensitivity, we turn to Fig. 4. We note that the electric field is higher at the amorphous - crystalline interface, when $N_{ss} = 3x10^{13}$ cm^{-2} than when $N_{ss} = 10^{11}$ cm^{-2} (Fig. 4a). This is because when the N-a-Si:H layer is joined to a P-c-Si wafer, with a high defect density on its surface, most of the electrons that flow from the N-side to the P-side during junction formation, to bring the thermodynamic equilibrium Fermi levels on either side to the same level, are trapped in these states. The space charge region on the P-c-Si wafer side is therefore localized near the surface and does not extend appreciably into the c-Si wafer. We therefore have a huge density of trapped electrons, a very high interface field (Fig. 4a),

N_{ss} on FS (cm^{-2})	J_{sc} (mA cm^{-2})	V_{oc} (mV)	FF	η(%)
10^{11}	37.50	672	0.770	19.40
$2x10^{12}$	38.33	586	0.658	14.79
$3x10^{13}$	38.14	463	0.545	9.65

Table 4. Calculated values of the solar cell output parameters J_{sc}, V_{oc}, FF and η, for different values of the defect density (N_{ss}) on that (front) surface of the crystalline silicon wafer through which light enters, indicating high sensitivity to the V_{oc} and FF. The defect density at the rear surface of the c-Si wafer is 10^{11} cm^{-2}.

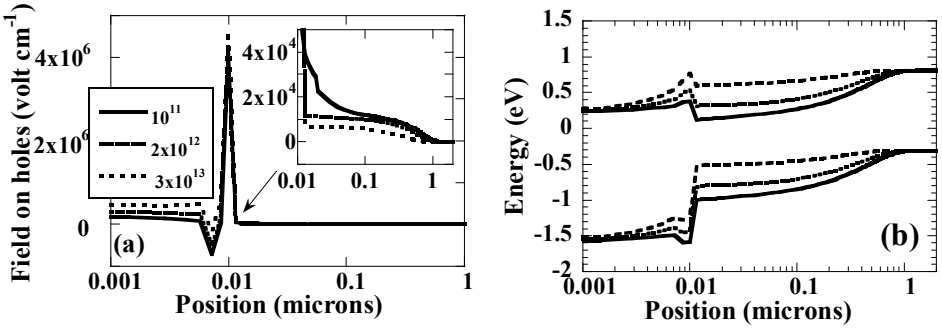

Fig. 4. Effect of changing the defect density (shown in units of cm^{-2}) on the front surface of the c-Si wafer under 100 mW cm^{-2} of AM1.5 light and 0 volts, on (a) the electric field (the inset shows the electric field on an expanded scale over the depletion region) and (b) the band diagram over the front part of the device.

and a collapse of the field over the adjacent depletion region of the c-Si wafer (Fig. 4a inset) for the case with N_{ss} = $3x10^{13}$ cm^{-2}. This results in the flattening of the energy bands in the totality of the P-type crystalline silicon wafer (Fig. 4b, dashed lines), and a consequent fall in V_{oc} and FF (Table 4). For the case of low N_{ss}, the space charge region on the P-c-Si wafer is not localized and more field exists up to the neutral zone of the c-Si wafer (Fig. 4a inset and band diagram in Fig. 5b, solid lines); resulting in higher V_{oc} and FF (Table 4).

4.3 Influence of the defect density on the rear surface of the c-Si wafer

Table 5 gives the calculated solar cell output parameters J_{sc}, V_{oc}, FF and efficiency for different values of the defect density (N_{ss}) on the rear surface of the c-Si wafer (away from the side where light enters). We have again varied N_{ss} between 10^{11} cm^{-2} and $3x10^{13}$ cm^{-2}, but this time the largest effect is on the fill factor and the short-circuit current density, as seen from Table 5 and Fig. 5 (a). In order to understand why, we have traced the band diagrams for different N_{ss} on the RS, with the N_{ss} at the FS held at 10^{11} cm^{-2} (Fig. 5b). We find that the band bending over the depletion region has completely disappeared for the highest value of N_{ss} ($3x10^{13}$ cm^{-2}) at RS. From our modeling calculations we also note that up to a defect density of ~10^{12} cm^{-2} at RS, the solar cell output parameters do not deteriorate appreciably. For higher values of N_{ss} the decrease in J_{sc} and FF in particular, is extremely rapid, the sensitivity to V_{oc} being relatively small. Experimentally also it has been found that whether or not an intrinsic passivating layer is deposited on the rear face of the P-type c-Si wafer, the

solar cell output is little affected. From this we may conclude that the defect density on the back wafer surface in the experimental as-deposited condition is probably ≤ 10^{12} cm^{-2}, as also obtained by modeling the experimental characteristics (Table 2).

N_{ss} on RS (cm^{-2})	J_{sc} (mA cm^{-2})	V_{oc} (mV)	FF	η(%)
10^{11}	37.50	672	0.770	19.40
10^{12}	37.48	662	0.752	18.66
$2x10^{12}$	37.34	625	0.666	15.54
$3x10^{13}$	5.47	572	0.156	0.49

Table 5. Calculated values of the solar cell output parameters for different values of the defect density (N_{ss}) on that (rear) surface of the crystalline silicon wafer that is away from the incoming light, indicating that the maximum sensitivity is to the short circuit current density and fill factor. The defect density at the front surface of the c-Si wafer is 10^{11} cm^{-2}.

In order to understand the sensitivity of the solar cell output to N_{ss} on the RS, we turn to Fig. 6. We note that when N_{ss} on the rear c-Si wafer surface is highest ($3x10^{13}$ cm^{-2}), there is a huge concentration of trapped holes at the crystalline- amorphous interface on the c-Si wafer side where the high surface defect density exists (dashed line, Fig. 6a). The hole pile-up at the crystalline-amorphous interface slows down the arrival of holes to the back contact (the collector of holes), and encourages the back diffusion of photo-generated electrons in the absorber c-Si wafer. The result is that the electron current is negative over most of the device (Fig. 6b – electron current towards the back contact is negative according to our sign convention). Thus little electron current is collected at the front contact (the collector of electrons, Fig. 6b). In addition, the back-diffusing electrons recombine with the photo-generated holes over most of the absorber c-Si, resulting in poor hole current collection at the back contact. Thus J_{sc} and FF fall sharply for very high values of N_{ss} at RS. More details can be found in Datta et al (2008).

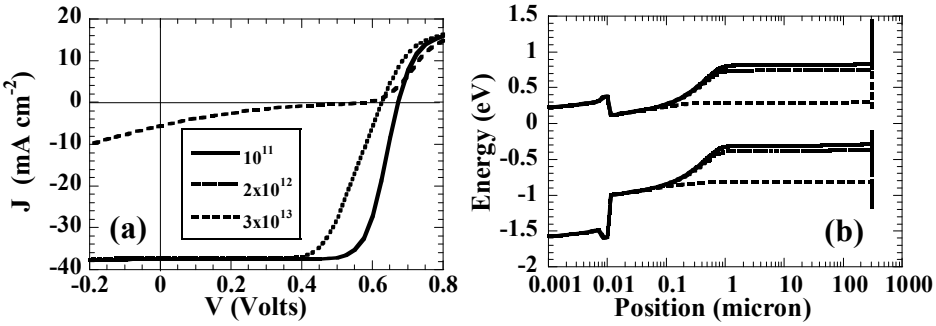

Fig. 5. Effect of changing the defect density (shown in units of cm^{-2}) on the rear surface of the c-Si wafer on (a) the illuminated current density versus voltage characteristics and (b) the band diagram at 0 volts as a function of position in the device under 100 mW cm^{-2} AM1.5 light. Results are shown for double heterojunction solar cells having a 4 nm P^{+}-a-SiC:H/ 19 nm P^{+}-a-Si:H BSF structure. The defect density on the front surface is 10^{11} cm^{-2} for all cases.

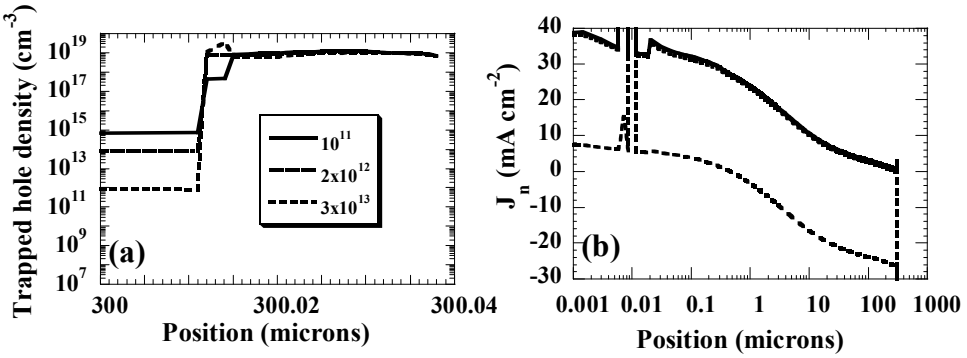

Fig. 6. Effect of changing the defect density (shown in units of cm^{-2}) on the rear surface of the c-Si wafer on (a) the trapped hole density, (b) the electron current density, J_n, and (c) the electric field on the holes. Results are shown for 100 mW cm^{-2} of AM1.5 light under short-circuit conditions.

5. Simulation of N-type HIT solar cells

5.1 Simulation of experimental results

Simulation of a range of experimental results on HIT cells developed by the Sanyo group and available in the literature (Maruyama et al, 2006, Takahama et al, 1992, Sawada et al, 1994, Taguchi et al, 2008) has been undertaken to extract typical parameters that characterize state-of-the-art HIT cells on N-type c-Si substrates, as well as to gain an insight into carrier transport and the general functioning of these cells. Both "front" HIT cells having an amorphous/ crystalline heterojunction on the emitter side only - where the light enters (Takahama et al, 1992), and "double" HIT cells having heterojunctions on both ends of the c-Si wafer (Maruyama et al, 2006, Sawada et al, 1994, Taguchi et al, 2008) have been simulated. The cells have the structure: ITO/ P-a-Si:H/ I-a-Si:H/ textured N-c-Si/ N-c-Si BSF/ metal (front HIT) (Takahama et al, 1992) and ITO/ P-a-Si:H/ I-a-Si:H/ textured N-c-Si/ I-a-Si:H/ N^{++}-a-Si:H/ metal (double HIT) (Maruyama et al, 2006, Sawada et al, 1994, Taguchi et al, 2008). In Taguchi et al (2008), after depositing the undoped and doped a-Si:H layers on both ends of the c-Si wafer, ITO films were sputtered on both sides, followed by screen-printed silver grid electrodes. Simulation of these cells (Maruyama et al, 2006, Takahama et al, 1992, Sawada et al, 1994) gives us an insight into the parameters that play a crucial role in improving HIT cell performance. On the other hand, the article by Taguchi et al (2008) gives the temperature dependence of the dark current density - voltage characteristics and the solar cell output parameters as a function of the thickness of the intrinsic amorphous layer sandwiched between the emitter P-a-Si:H and the main absorber N-c-Si. A study of the temperature dependence of the dark J-V characteristics is particularly important to understand the carrier transport mechanism in these devices. The parameters extracted by such modeling (Table 3) will be used in the following sections to calculate the sensitivity of the solar cell performance to various controlling factors.

In Table 6 we compare our simulation and experimental results of various HIT cells on N-type c-Si substrates (Takahama et al, 1992, Sawada et al, 1994, Maruyama et al, 2006). Modeling indicates that improvements in V_{oc} could be brought about (a) by going from a

HIT	Reference		N_{ss} (cm^{-2}) in defective layers	τ ms	V_{oc} **mV**	J_{sc} mA cm^{-2}	FF	η %
F	Takahama et al, 1992	E	– –	–	638	37.90	0.775	18.74
		M	FS- $4x10^{11}$	0.23	643	37.89	0.775	18.88
D-I	Swada et al, 1994	E	– –	–	644	39.40	0.790	20.05
		M	FS-$4x10^{11}$ RS -10^{11}	0.5	658	39.03	0.783	20.11
D-II	Maruyama et al, 2006	E	– –	1.20	718	38.52	0.790	21.85
		M	FS & RS - 10^{11}	2.00	713	38.60	0.797	21.93

Table 6. Comparison between measured (E): and modeled (M) solar cell output of front (F) and double (D) N-c-Si HIT cells with textured ITO front contact, developed by Sanyo over the years. "τ" is the lifetime of the minority carriers in the c-Si wafer.

front HIT to a double HIT structure, (b) by decreasing the defects on the front surface of the c-Si wafer that faces the emitter layer and (c) by improving the lifetime of the minority carriers in crystalline silicon. Results indicate that it is by decreasing N_{ss} on the front surface of the c-Si wafer, that the largest increase in V_{oc} could be achieved, without any fall in FF.

We next used ASDMP to simulate the experimental results of Taguchi et al (2008). Here we have concentrated on the effect of varying the thickness of the intrinsic amorphous silicon layer at the P-amorphous emitter/ N-c-Si heterojunction. The terminology "normal" has been used to represent the thickness of the front I-a-Si:H buffer layer in the cell that yields the highest efficiency (Table 7). Modeling reveals that the I-a-Si:H thickness for this case is 3 nm. The I-a-Si:H buffer layers (front) in the cells named "Half", "Double" and "Triple" by Taguchi et al (2008) have therefore been assigned thicknesses of 1.5 nm, 6 nm and 9 nm respectively in the simulations. Results of our simulation of the experimental light J-V characteristics (Taguchi et al, 2008) as a function of this I-a-Si:H layer thickness are given in Table 7 and the input parameters extracted by such modeling, and also of the dark J-V characteristics (Figs. 7a and 7b) and typical internal quantum efficiencies of Sanyo N-c-Si HIT cells (Fig. 7c, Maruyama et al, 2006), are given in Table 3 (the same table that contains the extracted parameters of P-type HIT cells). Since modeling does not consider the resistance of the contacts; these results had to be modified by taking into account the series resistance of the contacts. The addition of the series resistance did not modify V_{oc} and J_{sc} but allowed to perfectly match the experimental fill factor and therefore the efficiency of the Sanyo HIT solar cells (Taguchi et al, 2008). In Table 7 we show the solar cell output parameters as obtained directly by modeling, without resistive losses (which gives an upper limit for the FF and therefore the efficiency) and the values of the FF and efficiency after considering the constant series resistance (marked by astericks). This resistance, comprising resistive losses in the TCO, the silver grid and the contacts, was estimated by Taguchi et al (2008) to be ~2.8 mΩ.

Cell name	μ_n (μ_p) cm^2/volt-sec	I-a-Si:H thickness(nm)	N_{ss} (cm^{-2})		J_{sc} (mA cm^{-2})	V_{oc} (volts)	FF	η(%)
Half	30 (6)	1.5	$4x10^{11}$	E	37.4	0.699	0.776	20.3
				M	37.2	0.702	0.803	21.0
							0.775*	20.2*
Normal	25 (5)	3.0	$1.5x10^{11}$	E	37.2	0.711	0.773	20.4
				M	37.0	0.712	0.799	21.0
							0.774*	20.4*
Double	15 (3)	6.0	10^{10}	E	36.5	0.718	0.747	19.6
				M	36.7	0.717	0.766	20.2
							0.747*	19.7*
Triple	15 (3)	9.0	10^{10}	E	36.4	0.715	0.717	18.7
				M	36.6	0.714	0.750	19.6
							0.718*	18.8*

Table 7. Modeling (M) of the experimental (E) results of N-type HIT solar cells, having different thickness of the I-a-Si:H layer on the emitter side. N_{ss} is the defect density on that surface of the c-Si wafer that faces the emitter. The quantities given with astericks are the calculated values of FF and efficiency corrected for the series resistance of the contacts (2.8 m mΩ) (Taguchi et al, 2008).

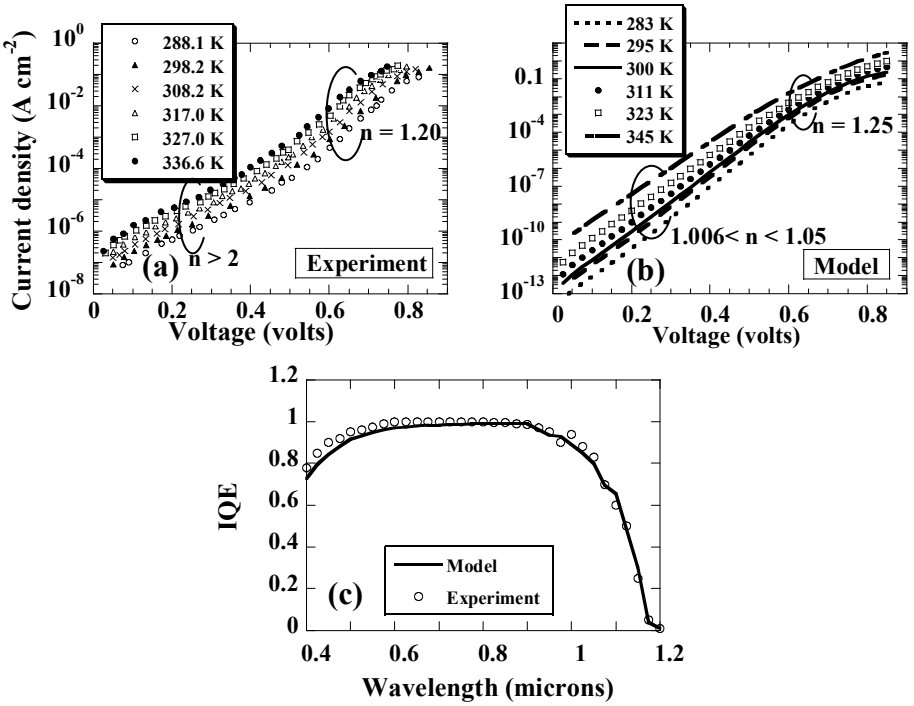

Fig. 7. (a) Experimental (Taguchi et al, 2008) and (b) simulated dark J-V characteristics of the cell with "Normal" thickness I-a-Si:H layer at the P-a-Si:H/ N-c-Si interface at various temperatures, and (c) the IQE of the same cell under AM1.5 illumination and 0 volts compared to the experimental IQE of a typical Sanyo cell (Maruyama et al,2004).

The dangling bond defect density in the I-a-Si:H layer, as extracted from modeling, is $9x10^{16}$ cm^{-3} and its Urbach enegy is 70 meV (Table 8). We have assumed the same values for these quantities, as well as of the capture cross-sections of the defect states inside the I-a-Si:H layer in all the cases of Table 7. Modeling indicates that in order to simulate the lower V_{oc}'s of the Taguchi et al (2008) cells "Normal" and "Half", the defect density on the surface of the c-Si wafer itself in these cases, must be higher (Table 7). We may justify this fact by assuming that a very thin buffer layer may not be as effective in passivating the defects on the surface of the c-Si wafer as a thicker buffer layer. In Table 7, we also had to assume higher carrier motilities in the front amorphous layers for the cases Half and Normal to match both the higher FF and lower V_{oc} for these cases. Increasing carrier mobilities over the front amorphous layers improves hole collection and therefore the FF. However, higher electron mobility allows more electrons to recto-diffuse towards the front contact (collector of photo-generated holes) and recombine with holes, thus reducing V_{oc}. However the main reason for the lower V_{oc} for thinner I-a-Si:H layers (Half and Normal) is our assumption of higher surface defect density on the c-Si wafer in these cases (Table 7).

The experimental dark J-V characteristics of the cell "Normal" is shown in Fig. 7 (a) and the model curves in Fig. 7 (b). The diode ideality factor, n, calculated in the voltage range 0.4 volts≤ V< 0.8 volts, from the model dark characteristics is 1.25 and compares well with the experimental value of 1.2. This value of "n" indicates that it is the diffusion current that dominates transport in this voltage range for N-c-Si HIT cells, as is also the case for homojunction c-Si solar cells. On the other hand, in the voltage range 0.1 volts< V< 0.4 volts, "n" calculated from the modeling data (Fig. 7b) is ~1, which indicates that the conductivity continues to be dominated by diffusion. The value of the slope, calculated from the experimental curves of Taguchi et al (2008) in the voltage range 0.1 volts < V < 0.4 is smaller than that of the recombination current model and remained almost constant for each temperature. The corresponding value of "n" derived from the experimental curves is greater than 2 (Fig. 7a). Taguchi et al (2008) therefore assumed that this is tunneling-limited current. If the value of "n" extracted from the experimental curves, had been due to current dominated by recombination, ASDMP would also have been able to reproduce this value of 'n', since the recombination current model is included in ASDMP. In fact ASDMP has already been used to successfully model forward and dark reverse bias characteristics of a-Si:H based PIN solar cells, where recombination plays a dominant role (Tchakarov et al, 2003). The fact that the value of "n" calculated from the ASDMP-generated dark J-V curves is ~1, while that from experiments is different, indicates that the current over this region is dominated by a phenomenon *not* taken account of by ASDMP (e.g. tunneling). Over this voltage region therefore the current could be dominated by the tunneling of electrons. However, as pointed out by Taguchi et al (2008), "the current density in this region is sufficiently low compared to the levels of short-circuit current density and does not affect solar cell performance". It therefore appears that cell performance under AM1 or AM1.5 light is not affected by tunnelling of electrons, although this phenomenon probably exists for V< 0.4 volts.

Fig. 8 shows the temperature dependence of the solar cell output parameters. We have made the comparison between experiments (Taguchi et al, 2008) and modeling, after taking account of the series resistance of the contacts that is independent of temperature. As the temperature decreases, carrier density decreases. It means less carrier recombination and therefore a higher V_{oc} at lower temperatures (Fig. 8a). However lower carrier density at

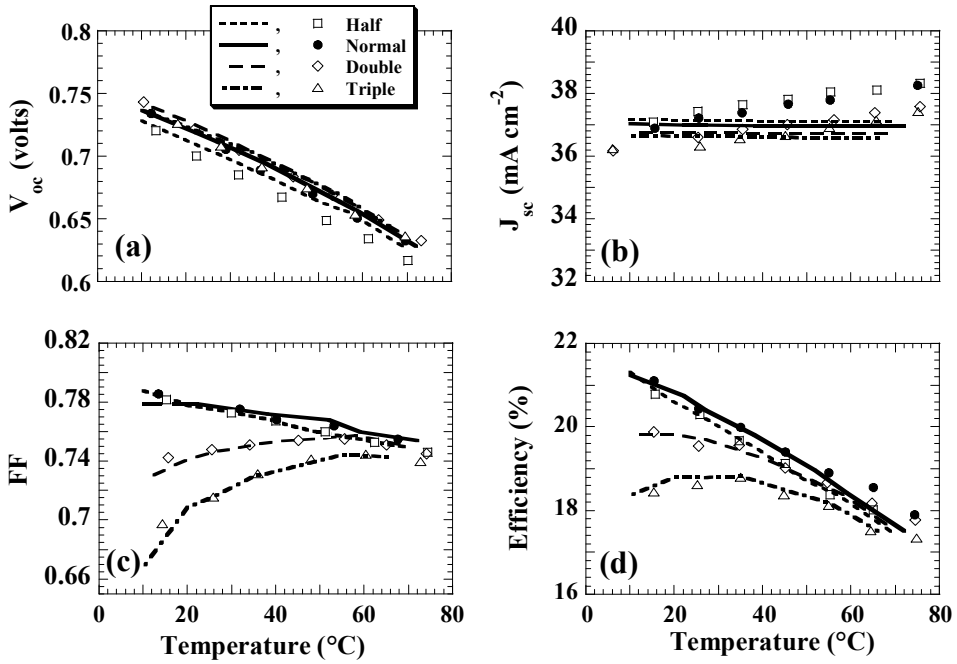

Fig. 8. Variation of (a) V_{oc}, (b) J_{sc}, (c) FF and (d) Efficiency as a function of temperature in N-c-Si HIT solar cells having different thickness of the undoped a-Si:H layer (half, normal, double, triple) at the P-a-Si:H/ N-c-Si interface. The lines are modeling results, while symbols correspond to measured data.

lower temperatures, also means that the cell is now more resistive, resulting in a fall in the FF for the cells "double" and "triple" (Fig. 8c), where performance is dominated by the undoped a-Si:H layer. Also, for the value of the band gap assumed for the I-a-Si:H layer (Table 8), the holes are able to overcome the positive field barrier at the a-Si/ c-Si interface by thermionic emission to get collected at the front contact. Thermionic emission decreases at lower temperatures, resulting in a loss of FF for cells "double" and "triple". For cells "Normal" and "Half", performance is dominated by the temperature-independent resistance of the contacts; therefore no fall in FF is seen. Finally Fig. 8 (b), indicates that the calculated J_{sc} is constant with temperature, while the measured J_{sc} increases slightly. This is because the model does not take account of the temperature dependence of the band gap and absorption coefficient of the materials.

5.2 Effect of I-a-Si:H buffer layers on the performance of N- type HIT solar cells

HIT solar cells give efficiencies comparable to those of c-Si cells because of the amazing passivating properties of the intrinsic a-Si:H layers. In fact it is this layer that gives this group of solar cells its name – "HIT". We have already discussed that it is very effective in passivating the defects on the surface the c-Si wafer. However, it must be kept as thin as possible, as it reduces the fill factor when thick (Table 7). We have next studied the effect on

solar cell performance of varying the defect density in this layer itself. For this purpose, we have assumed its thickness to be 6 nm (as in case "Double") where the best passivation of N_{ss} has been attained (Table 7). An increase in the defect density in the I-a-Si:H layer may affect the defect density (N_{ss}) on c-Si, but in this study we assume N_{ss} to be constant. We have found (Rahmouni et al, 2010) that unless the defect density of this intrinsic layer is greater than $3x10^{17}$ cm^{-3}, no significant loss of cell performance occurs. Similar conclusions have been reached in the case of HIT cells on P-type c-Si wafers.

5.3 Effect of the defect density on the front and rear faces of the N-type c-Si wafer

The sensitivity of the solar cell output of HIT cells on N-type wafers to the surface defect density (N_{ss}) at the amorphous/crystalline interface is given in Table 9. All aspects of the solar cell output appear to be highly sensitive to the N_{ss} on the front surface (on the side of the emitter layer) of the N-type c-Si wafer; however the sensitivity to N_{ss} on the rear face is weak and is limited to the condition when these defects are very high. We have also given in Table 8, the values of the corresponding recombination speeds at the a-Si:H /c-Si front and the c-Si/a-Si:H rear heterojunctions, as calculated by ASDMP, under AM1.5 illumination and short circuit condition. We find that for a well-passivated front interface ($N_{ss} \leq \sim 3x10^{11}$ cm^{-2}) the recombination speed at this heterojunction is less than 10 cm/sec (Table 8), in good agreement with measured interface recombination speeds (Dauwe et al, 2002).

N_{ss} at front (DL) (cm^{-2})	S_p at front (DL) (cm/s)	N_{ss} at back (DL) (cm^{-2})	S_n at back (DL) (cm/s)	Jsc (mA cm^{-2})	V_{oc} (volts)	FF	η(%)
10^{10}	3.62			36.96	0.720	0.801	21.32
$1.5x10^{11}$	4.20			37.00	0.712	0.799	21.03
10^{12}	24.73	10^{10}	$2.89x10^{4}$	37.24	0.636	0.695	16.46
$2x10^{12}$	202.62			37.37	0.596	0.470	10.47
10^{13}	$1.16x10^{3}$			18.83	0.544	0.160	1.64
$1.5x10^{11}$	4.20	10^{10}	$2.89x10^{4}$	37.00	0.712	0.799	21.03
		10^{11}	$2.37x10^{4}$	36.99	0.711	0.799	21.01
		10^{12}	$1.95x10^{4}$	36.98	0.696	0.797	20.51
		10^{13}	$1.00x10^{4}$	35.45	0.609	0.779	16.82

Table 8. Sensitivity of the solar cell output to the defect density (N_{ss}) in thin surface layers (DL) on the front and rear faces of the c-Si wafer in N type double HIT solar cells. The P-layer thickness is 6.5 nm. The recombination speeds of holes (S_p - at the front DL) and electrons (S_n – at the rear DL), calculated under AM 1.5 light and 0 volts, are also shown.

In Fig.9 (a) we plot the light J-V characteristics and in Fig. 9 (b) the band diagram for various values of N_{ss} on the front face of the c-Si wafer. We find that for a very high defect density on the surface of the c-Si wafer, the depletion region in the N-c-Si wafer completely vanishes, while the emitter P-layer is depleted (Fig. 9b). With a high N_{ss} on the c-Si wafer, the holes left behind by the electrons flowing into the P-layer during junction formation, are localized on its surface, leading to a high negative field on the wafer surface and little field penetration into its bulk (Fig. 10a). Hence the near absence of the depletion zone in N-c-Si and a strong fall in V_{oc} for the highest N_{ss} (10^{13} cm^{-2}).

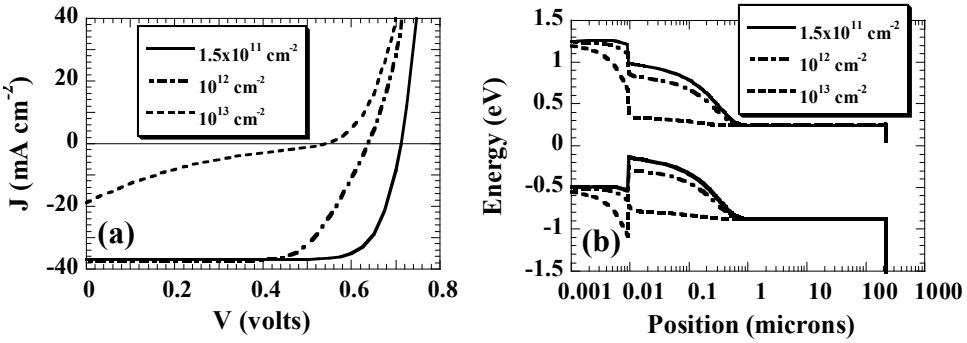

Fig. 9. (a) The light J-V characteristics and (b) the band diagram under AM1.5 light bias and 0 volts for different values of N_{ss} on the front face of the N type c-Si wafer.

In Fig. 10 (b) we plot the trapped hole population over the front part in N-c-Si double HIT cells under AM1.5 bias light at 0 volts. We note that when N_{ss} on the front c-Si wafer surface is the highest (10^{13} cm^{-2}), there is a huge concentration of holes at the amorphous / crystalline (a-c) interface on the c-Si wafer side, where the high surface defect density exists (dashed line, Fig. 10b).

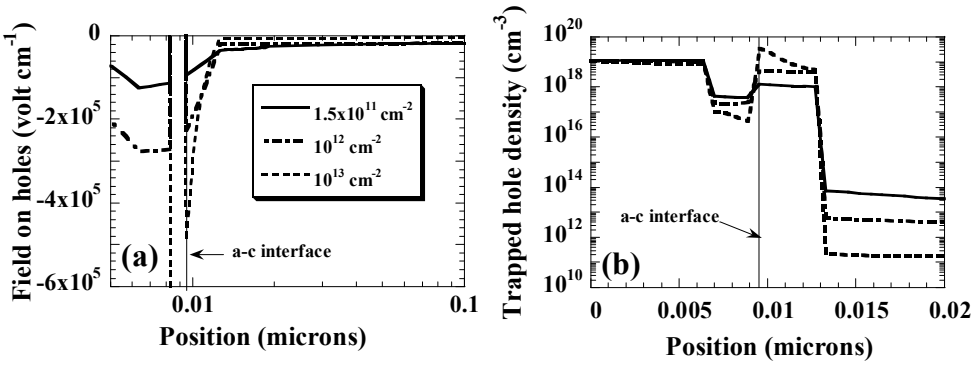

Fig. 10. Plots of (a) the electric field on the holes and (b) the trapped hole density over the front part of the device as a function of position in the entire device under illumination and short-circuit conditions, in N-c-Si HIT cells for different densities of defects on the front face of the c-Si wafer. The amorphous/crystalline (a-c) interface is indicated on (a) and (b).

The hole pile-up at the amorphous / crystalline interface slows down the arrival of holes to the front contact (the collector of holes), and attracts photo-generated electrons, i.e., encourages their back diffusion towards the front contact. The result is that the electrns back-diffuse towards the front contact and recombine with the photo-generated holes resulting in poor carrier collection (Rahmouni et al, 2010). Thus J_{sc} and FF fall sharply for high values of N_{ss} on the front surface of c-Si (Table 8). In fact we may arrive at the same conclusion also from Fig. 9 (b), which shows that for $N_{ss} = 10^{13}$ cm^{-2}, there is almost no band bending or electric field in the c-Si wafer (the main absorber layer) so that carriers cannot be collected, resulting in the general degradation of all aspects of solar cell performance.

On the other hand Table 8 indicates that there is little sensitivity of the solar cell output to the defect states on the rear face of the wafer, except at the highest value of N_{ss}. To explain this fact, we note that the recombination over the rear region is determined by the number of holes (minority carriers) that can back diffuse to reach the defective layer. Not many succeed in doing so, since the high negative field due to the large valence band discontinuity at the c-Si/ a-Si rear interface pushes the holes in the right direction, in other words, towards the front contact. Therefore the defects over this region cannot serve as efficient channels for recombination, and there is no large difference between the recombination through these states for different values of N_{ss} (Table 8). Moreover the conduction band discontinuity at the c-Si/ a-Si interface is about half that of the valence band discontinuity. Since the mobility of electrons, relative to that of holes, is also much higher, clearly this reverse field due to the conduction band discontinuity poses little difficulty for electron collection even when the defect density at this point is high, except when $N_{ss} \geq 10^{13}$ cm^{-2}, from which point the solar cell performance deteriorates.

6. Comparative study of the performances of HIT solar cells on P- and N-type c-Si wafers

Using parameters extracted by our modeling (given in Tables 3), we have made a comparative study between the performances of HIT solar cells on 300 μm thick textured P- and N-type c-Si wafers (for more details refer to Datta et al, 2010).

6.1 Sensitivity of amorphous/crystalline band discontinuity in the performances of HIT solar cells

Since the band gap, activation energy of the amorphous layers and the band discontinuities at the amorphous/crystalline interface are interlinked, we treat these sensitivity calculations together. For HIT cells on P-c-Si, the large valence band discontinuity (ΔE_v) on the emitter side prevents the back-diffusion of holes and has a beneficial effect. Keeping this constant, we varied the mobility gap and therefore the conduction band discontinuity (ΔE_c) on the emitter side. We find that a ΔE_c upto 0.3 eV, does not impede electron collection, but instead brings up both J_{sc} and V_{oc}, due to an improved built in ptential (V_{bi}).

However high ΔE_v at the crystalline/amorphous (c-a) interface on the BSF side of P-c-Si double HIT cells (Table 9), impedes hole collection, resulting in a pile up of holes on the c-Si side of this band discontinuity (Fig. 11a) and a consequent sharp fall in the FF and S-shaped J-V characteristics for high ΔE_v, especially when the activation energy of the P-a-Si:H layer is also high (Fig. 11b).

E_μ (P) (eV)	E_{ac} (eV)	ΔE_v (eV)	J_{sc} (mA cm^{-2})	V_{oc} (mV)	FF	η %
1.75	0.3	0.41	36.70	649	0.810	19.28
1.75	0.4	0.41	36.69	647	0.688	16.34
1.80	0.3	0.46	36.70	649	0.807	19.21
1.90	0.3	0.56	36.70	649	0.762	18.14
1.90	0.4	0.56	36.68	649	0.484	11.51
1.98	0.4	0.64	27.45	649	0.171	3.04

Table 9. Variation of solar cell output with mobility gap (E_μ), activation energy (E_{ac}) and ΔE_v (P-c-Si/P-a-Si:H BSF interface) in double P-c-Si HIT solar cells. ΔE_c is held constant at 0.22eV.

It is for this reason that a transition from a front to a double HIT structure does not appreciably improve cell performance for P-c-Si HIT cells. The accumulated holes at the c-a interface, furthermore, repel the approaching holes and encourage photo-generated electron back diffusion, resulting in increased recombination, that reduces even J_{sc} for the highest ΔE_v (Table 9, Fig. 11b). Finally, for high hole pile-up, the amorphous BSF is screened from the rest of the device, so that the large variation of its band gap and activation energy (Table 9) fails to alter the V_{oc} of the device. The best double HIT performance is attained when the mobility gap (ΔE_μ) of the amorphous BSF P-layer is ≤ 1.80 eV and E_{ac} = 0.3 eV (Table 9).

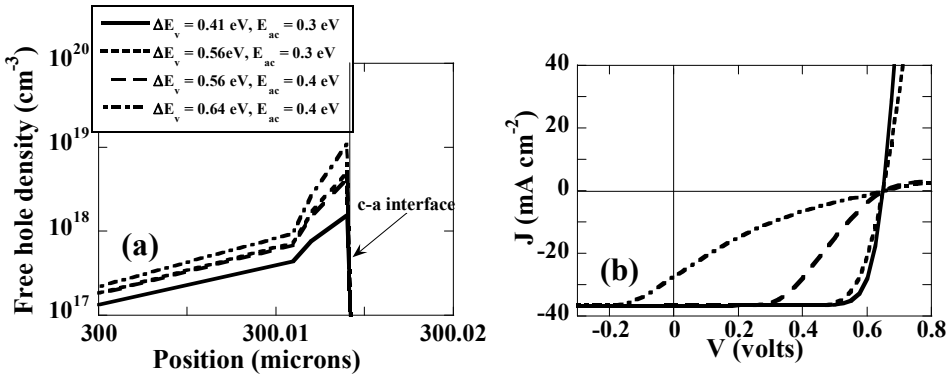

Fig. 11. Variation of (a) the free hole population near the c-Si/ amorphous BSF interface and (b) the light J-V characteristics for different valence band discontinuities (ΔE_v) and activation energies (E_{ac}) of the P-BSF layer in double P-c-Si HIT solar cells. ΔE_c = 0.22eV in all cases.

Table 10 shows the effect of the variation of the emitter P-layer mobility gap, activation energy and the valence band discontinuity at the a-c interface on N-c-Si double HIT cell performance.

E_μ (P) (eV)	E_{ac} (eV)	ΔE_v (eV)	J_{sc} (mA cm^{-2})	V_{oc} (mV)	FF	η (%)
1.75	0.3	0.41	38.06	670	0.818	20.86
1.75	0.4	0.41	38.14	652	0.681	16.93
1.80	0.3	0.46	38.10	671	0.811	20.75
1.90	0.3	0.56	38.22	677	0.705	18.25
1.90	0.4	0.56	38.38	674	0.463	11.98
1.98	0.4	0.64	28.18	732	0.184	3.79

Table 10. Variation of solar cell output parameters with mobility gap (E_μ), activation energy (E_{ac}), and ΔE_v at the emitter P-a-Si:H/c-Si interface in double N-c-Si HIT solar cells. ΔE_c is held constant at 0.22eV.

Table 10 indicates that for valence band offsets up to 0.51 eV, and E_{ac} (P) ≤ 0.3 eV, the FF is high, indicating that the majority of the holes photo-generated inside the c-Si wafer, can surmount the positive field barrier due to the a-Si/ c-Si valence band discontinuity by

thermionic emission and get collected at the front ITO/ P-a-Si:H contact. However solar cell performance deteriorates both with increasing band gap and increasing E_{ac} of the P-layer. The latter is only to be expected as it reduces the built-in potential.

Fig. 12 (a) shows the effect on the energy band diagram of increasing the P-layer band gap (therefore of increasing ΔE_v, since ΔE_c is held constant) and the activation energy. Increasing ΔE_v at the P-a-Si:H/N-c-Si interface results in hole accumulation and therefore a fall in FF for $\Delta E_v \geq 0.56$ eV, for a P-layer activation energy of ~0.3 eV, due to the reverse field it generates; that is further accentuated when E_{ac} is high (Table 10). van Cleef et al (1998 a,b) have also shown that for a P-layer doping density of $9x10^{18}$ cm^{-3} (same as ours – Table 3, giving E_{ac} = 0.3 eV) and for ΔE_v = 0.43 eV, normal J-V characteristics are achieved at room temperature and AM1.5 illumination, and that "S-shaped" characteristics begin to develop at higher ΔE_v and E_{ac}. In our case, for $\Delta E_v \geq 0.60$ eV, Fig. 12(c) indicates that free holes accumulate over the entire c-Si wafer, resulting in a sharp reduction of the electric field and flat bands over the depletion region, on the side of the N-type c-Si wafer (Fig. 12b). This fact results in a sharp fall in the FF and conversion efficiency (Table 10). In fact under this condition, the strong accumulation of holes on c-Si, can partially deplete even the highly defective P-layer, resulting in a shift of the depletion region from c-Si to the amorphous emitter layer (Fig. 12a). This also means that the carriers can no longer be fully extracted at 0 volts, resulting in a fall in J_{sc} (Table 10). We have found that the current recovers to the normal value of ~36 mA cm^{-2} only at a reverse bias of 0.3volts (Datta et al, 2010). Modeling indicates that for improved performance of N-c-Si HIT cells, the valence band offset has to be reduced by a lower emitter band gap, unless the tunneling of holes exists.

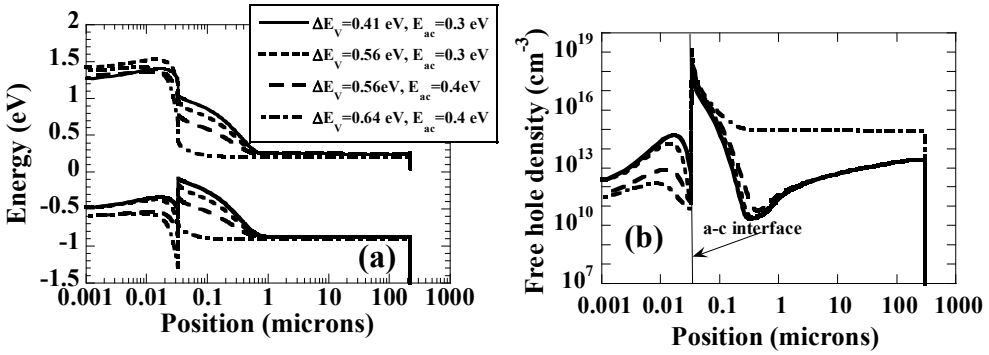

Fig. 12. Variation of (a) the band diagram under AM1.5 light and 0 volts and (b) the free hole population under the same conditions, as a function of position in the N-c-Si HIT device for different valence band discontinuities (ΔE_v) and activation energies (E_{ac}) of the emitter layer.

6.2 Sensitivity of the solar cell output to the front contact barrier height.

The front TCO/P-a-Si:H contact barrier height, ϕ_{b0} in N-type HIT cells is determined by the following expression:-

$$\phi_{b0} = E_{\mu}(P) - E_{ac}(P) - sbb\,, \tag{3}$$

where $E_{\mu}(P)$ and $E_{ac}(P)$ represent respectively the mobility band gap and the activation energy of the P-layer, and 'sbb' is the surface band bending due to a Schottky barrier at the TCO/P interface. With a change of the work function of the TCO, it is this 'sbb' that varies. In this section we study the dependence of the solar cell output to changes in this surface band bending. We hold the band gap and the activation energies of the P-layer constant at 1.75 eV and 0.3 eV respectively, so that the TCO work function has a direct effect on the front contact barrier height. The results are summarized in Fig. 15. For these sensitivity calculations we have chosen the thickness of the P-layer to be 15 nm (Rahmouni et al, 2010). Fig. 13 indicates that both V_{oc} and FF fall off for $\Phi_{b0} \leq 1.05$ eV.

We have also studied the effect of changing the rear P-a-Si:H BSF/TCO barrier height , ϕ_{bL}, in P-c-Si HIT cells. The variation in the current-density – voltage characteristics follow a similar pattern as Fig. 15.

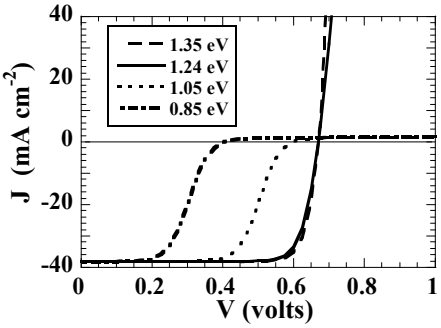

Fig. 13. The current density - voltage characteristics under AM1.5 light and 0 volts for different front contact barrier heights. The band gap, the activation energy and the thickness of the P-layer are held constant at 1.75 eV, 15 nm and 0.3 eV respectively, so that only surface band bending changes.

6.3 Relative influence of different parameters on the performance of HIT cells

In this section we make a comparative study of the influence on HIT cell performance, of the N_{ss} on the surface of the c-Si wafer, the lifetime (τ) of the minority carriers in c-Si, and the surface recombination speeds (SRS) of free carriers at the contacts. The sensitivity to the first two is shown in Table 11. For all the cases studied here, the P layer has an activation energy of 0.3 eV and a surface band bending 0.21 eV.

We note that when the defect density on the surfaces of the c-Si wafer is low, there is some sensitivity of the solar cell output to τ. In fact the conversion efficiency increases by ~3.22% and ~2.47% in double P-c-Si and N-c-Si HIT cells respectively as τ varies from 0.1 ms to 2.5 ms. By contrast there is a huge sensitivity to N_{ss}, as already noted in sections 4.2, 4.3 and 5.3; the performance of the HIT cell depending entirely on this quantity when it is high, with no sensitivity to τ (Table 11). The lone exception is the N_{ss} on the rear face of N-c-Si, to which solar cell output is relatively insensitive as already noted

Finally, the minority carrier SRS at the contacts, that regulates the back diffusion of carriers, has only a small influence in these double HIT cells. The majority carrier SRS does not affect cell performance up to a value of 10^3 cm/s, except the SRS of holes at the contact that is the

Type	N_{ss} (cm^{-2})		τ	J_{sc}	V_{oc}	FF	η
	Front	Rear	(ms)	(mA cm^{-2})	(mV)		(%)
P-c-Si	$4x10^{11}$	10^{11}	0.1	36.22	604	0.794	17.37
			0.5	36.61	649	0.808	19.19
			2.5	36.68	687	0.817	20.59
	$3x10^{13}$	10^{11}	0.5	37.24	472	0.626	11.00
			2.5	37.17	471	0.626	10.96
	$4x10^{11}$	$3x10^{13}$	0.5	5.68	572	0.154	0.50
			2.5	5.59	572	0.153	0.49
N-c-Si	$4x10^{11}$	10^{11}	0.1	38.39	631	0.767	18.58
			0.5	39.03	658	0.783	20.13
			2.5	39.20	678	0.792	21.05
	$3x10^{13}$	10^{11}	0.5	11.54	537	0.208	1.29
			2.5	11.58	537	0.207	1.29
	$4x10^{11}$	$3x10^{13}$	0.5	37.04	615	0.763	17.39
			2.5	37.08	616	0.763	17.44

Table 11. Sensitivity of double HIT solar cell output parameters to N_{ss} on the front and rear surfaces of the c-Si wafer and minority carrier life-time (τ).

hole-collector. Hole collection (at the rear contact in P-c-Si HIT and at the front in N-c-Si HIT) is already somewhat impeded by the large valence band discontinuity at the amorphous/ crystalline interface and the lower mobility of holes relative to electrons; hence a low value of SRS of holes at the contacts is expected to have a disastrous influence on hole collection. The effect of lowering S_{p0} for N-c-Si HIT cells is shown in Fig. 14, and is seen to lead to S-shaped J-V characteristics with a sharp fall in the FF when reduced to ≤ 10^4 cm/sec. In fact when sputtering ITO onto c-Si substrates coated with a-Si:H (intrinsic and doped) films, we sometimes obtain a rather degraded P/ITO interface, where the surface recombination speed is probably reduced. Therefore, Fig. 14 indicates that ITO deposition conditions can also be critical for good solar cell performance.

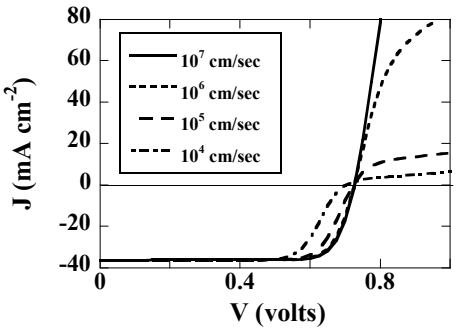

Fig. 14. The sensitivity of the illuminated J-V characteristic under AM1.5 light and short-circuit condition, to the surface recombination speed of the holes at the ITO/P front contact.

7. Conclusions

We have studied the performance of HIT cells on P-and N-type c-Si wafers, using detailed computer modeling. In order to arrive at a realistic set of parameters that characterize these cells, we have modeled several experimental results. We find that the major breakthroughs in improving the performance of these cells having textured N-type c-Si as the absorber layer, come from the introduction of an amorphous BSF layer, by passivating the defects on the c-Si wafer surface and, to a lesser extent, by improving the lifetime of the minority carriers in the c-Si wafer (Table 6).

Modeling indicates that both types of HIT cell output is very sensitive to the defects on the surface of the c-Si wafer, and good passivation of these defects is the key to attaining high efficiency in these structures. An exception to this rule is the defects on the rear face of c-Si in N-type HIT cells, to which there is not much sensitivity. The amorphous/crystalline valence band discontinuity also has a strong impact. In particular, large ΔE_v at the emitter P-a-Si:H/N-c-Si contact leads to S-shaped J-V characteristics, unless tunneling of holes takes place; while that at the P-c-Si/P-BSF contact reduces the FF in double P-c-Si HIT cells. It is for this reason that a transition from a front to double HIT structure on P-c-Si does not produce the spectacular improvement observed for N-type HIT cells (Table 6). Solar cell output is also influenced to some extent by the minority carrier lifetime in c-Si. In Table 12 we compare the performance of a P-type and an N-type HIT cell, with low N_{ss} on the wafer surface, and realistic input parameters. We find that the N-type HIT cell shows better performance than a P-c-Si HIT cell with a higher V_{oc} and conversion efficiency, because of a higher built-in potential in the former. However, the fill factor of N-c-Si HIT cells is lower than in P-type HIT cells due to the assumption of $\Delta E_v > \Delta E_c$, resulting in the holes facing more difficulty in getting collected at the front contact in the former case. This fact has also been pointed out by other workers (Stangl et al, 2001, Froitzheim et al, 2002). In P-type HIT cells, the electrons are collected at the front contact and have to overcome the relatively low ΔE_c at the crystalline/amorphous interface so that its FF is higher than in N-c-Si HIT.

Type	J_{sc} (mA cm^{-2})	V_{oc} (mV)	FF	η (%)
Double HIT on P-c-Si	37.76	694	0.828	21.72
Double HIT on N-c-Si	38.89	701	0.814	22.21

Table 12. Comparison of the performance of P-type and N-type double HIT cells, with optimized parameters. The life time of minority carriers in the c-Si wafer in both cases is 2.5 ms and its doping 10^{16} cm^{-3}.

8. Acknowledgements

The authors wish to express their gratitude to Prof. Pere Roca i Cabarrocas of LPICM, Ecole Polytechnique, Palaiseau, France for providing all the experimental results on "HIT" cells on P-types wafers, that have been simulated in this article. We are also grateful to him for many in-depth discussions and constant encouragement during the course of this work. The authors also wish to thank Prof. C. Baliff, of IMT, University of Neuchâtel, Switzerland, M. Nath of the Energy Research Unit, IACS, Kolkata, India and J. Damon-Lacoste of TOTAL, S. A. for many helpful discussions.

9. References

Arch, J. K.; Rubinelli, F. A.; Hou, J. Y. and Fonash, S. (1991) Computer analysis of the role of p-layer quality, thickness, transport mechanisms, and contact barrier height in the performance of hydrogenated amorphous silicon p-i-n solar cells, *Journal of Applied Physics* Vol.69, No. 10(May, 1991) pp 7057 -7066, ISSN 0021-8979.

Basore, P. A. (1990), Numerical modeling of textured silicon solar cells using PC-1D IEEE Transaction on Electron Devices, Vol 37, No. 2 (February, 1990) pp. 337 – 343, ISSN 0018-9383 .

Clugston, D.A and Basore P. A. (1997), PC1D version 5: 32-bit solar cell modeling on personal computers, *Proceedings of 26th IEEE Photovoltaic Specialists Conference,* pp. 207- 201, ISBN: 0-7803-3767-0, Anaheim, USA, 1997, September 29-October 3.

Chatterjee, P. (1992), Computer modeling of the dependence of the J-V characteristics of a-Si:H solar cells on the front contact barrier height and gap state density, Technical Digest of International PVSEC-6, New Delhi, India, Feb. 10-14 (1992) pp 329-334.

Chatterjee P. (1994), Photovoltaic performance of a-Si:H homojunction p-i-n solar cells: A computer simulation study, *Journal of Applied Physics* , Vol 76 No.2 (July, 1994) pp 1301-1313, ISSN 0021-8979.

Chatterjee, P. (1996), A computer analysis of the effect of a wide-band-gap emitter layer on the performance of a-Si:H-based heterojunction solar cells, *Journal of Applied Physics*, Vol 79, No 9 (May, 1996) pp 7339-7347, ISSN (print) 0021-8979.

Chatterjee, P.; Leblanc, F.;Favre; M. and Perrin, J. (1996), A global electrical-optical model of thin film solar cells on textured substrates, *Mat. Res. Soc. Symp. Proc.* 426 (1996) pp 593-598.

Datta A., Damon-Lacoste J., Roca i Cabarrocas P., Chatterjee P. (2008), Defect states on the surfaces of a P-type c-Si wafer and how they control the performance of a double heterojunction solar cell, *Solar energy Materials and Solar Cells*, Vol 92 (August, 2008) pp 1500-1507, ISSN 0927-0248.

Datta, A.; Damon-Lacoste, J.; Nath, M.; Roca i Cabarrocas, P. andChatterjee P. (2009), Dominant role of interfaces in solar cells with N-a-Si:H/P-c-Si heterojunction with intrinsic thin layer, *Materials Science and Engineering B,* Vol 15-160 (2009), 10-13.

Datta, A.; Rahmouni, M.; Nath, M.; Boubekri, R.; RocaiCabarrocas, P. and Chatterjee, P. (2010) , Insights gained from computer modeling of heterojunction with instrinsic thin layer ''HIT'' solar cells, *Solar energy Materials and Solar Cells,* Vol 94, (April, 2010) pp 1457-1462, ISSN 0927-0248.

Damon-Lacoste J., Ph. D Thesis, Ecole Polytechnique Paris, 2007.

Dauwe, S; Schmidt, J. and Hezel, R.,2002, Very low surface recombination velocities on p- and n-type silicon wafers passivated with hydrogenated amorphous silicon films, *Proceedings of 29th IEEE Photovoltaic Specialists Conference*, pp.1246 – 1249, ISBN 0-7803-7471-1, New Orleans, USA, 2002, May 19-24.

Froitzheim, A.; Stangl, R.; Elstner, L.; Schmidt, M. and Fuhs, W. (2002), Interface recombination in amorphous/crystalline silicon solar cells, a simulation study, Proceedings *of 29th IEEE Photovoltaic Specialists' Conf.*,19-24 May (2002), New Orleans, USA, pp. 1238-1241.

Fuhs, W.; Niemann, K. and Stuke, J. (1994), Heterojunctions of amorphous silicon and silicon single crystals, *AIP Conference Proceedings,* Vol 20 (May 1974) pp 345-350.

Fujiwara, H.; Sai, H. and Kondo M. (2009), Crystalline Si Heterojunction Solar Cells with the Double Heterostructure of Hydrogenated Amorphous Silicon Oxide, *Japanese Journal of Applied Physics* Vol 48 (June 2009) pp 064506 -1-4, ISSN 0021-4922.

Guha, S.; Yang, J.; Pawlikiewicz, A.; Glatfelter, T., Ross, R. and Ovshinsky, S. R . (1989), Band-gap profiling for Improving the efficiency of amorphous silicon alloy solar cells Applied Physics Letters Vol 54, No 23 (June 1989) pp 2330-2332, ISSN 0021-8979.

Hack, M. and Schur, M (1985)., Physics of amorphous silicon alloy p-I-n solar cells, *Journal of Applied Physics,* Vol 58 (1985) pp 997-1020, ISSN 0021-8979.

Kanevce, A. and Metzger W. K. (2009), The role of amorphous silicon and tunneling in heterojunction with intrinsic thin layer (HIT) solar cells, *Journal of Applied Physics*, Vol 105, No. 9, (May,2009), pp. 094507-1-7, ISSN 0021-8979.

Leblanc, F.; Perrin, J. and Schmitt, J. (1994), Numerical modeling of the optical properties of hydrogenated amorphous-silicon-based p-i-n solar cells deposited on rough transparent conducting oxide substrate, *Journal of Applied Physics* Vol 75, No.2 (January 1994) pp 1074-1087, ISSN 0021-8979.

Maruyama, E.; Terakawa, A.; Taguchi, M.; Yoshimine, Y.; Ide, D.; Baba, T.; Shima, M.; Sakata, H. and Tanaka, M. (2006), *Sanyo's Challenges to the Development of High-efficiency HIT Solar Cells and the Expansion of HIT Business, Proceedings 4th World Conf. on Photovoltais Solar Energy Conversion,* Hawaii, USA, 9-12 May (2006).

McElheny, P.; Arch, J. K.; Lin, H.-S. and Fonash, S., Range of validity of the surface-photovoltage diffusion length measurement: A computer simulation *Journal of Applied Physics*, Vol 64 No. 3 (August 1988) pp 1254-1265, ISSN 0021-8979.

Meier, D.L.; Page, M.R.; Iwaniczko, E.; Xu, Y.; Wang, Q. and Branz, H.M. (2007), Determination of surface recombination velocities for thermal oxide and amorphous silicon on float zone silicon, *Proceedings of the 17th Workshop on Crystalline Silicon Solar Cells and Modules*, pp.214-217, Vail, CO, USA, 2007.

Nath, M; Chatterjee, P.; Damon-Lacoste, J. and Roca i Cabarrocas, P. (2008), Criteria for improved open-circuit voltage in *a*-Si:H(*N*)/*c*-Si(*P*) front heterojunction with intrinsic thin layer solar cells*, Journal of Applied Physsics* , Vol 103 (February, 2008) pp 034506-1-9, ISSN 0021-8979.

Olibet, S.; Vallat-Sauvain E.; Fesquet, L.; Monachon, C.; Hessler-Wyser, A.; Damon-Lacoste, J.; De Wolf, S. and Ballif, C. (2010), Properties of Interfaces in Amorphous/Crystalline Silicon Heterojunctions, *Physics Status Solidi A,* Vol 207, No. 3 (January, 2010)pp 651–656, ISSN 1862-6300.

Olibet, S.; Vallat-Sauvain, E. and Ballif, C. (2007), Model for a-Si:H/c-Si interface recombination based on the amphoteric nature of silicon dangling bonds, *Physical Review B*, Vol 76, No 3, (July, 2007), pp 035326-1 – 14, ISSN 1098-0121.

Osuda, K.; Okamoto, H. and Hamakawa, Y. (1983), Amorphous Si/Polycrystalline Si stacked solar cells having more than 12% conversion efficiency,*Japanese Journal of Applied Physics*, Vol 22, No.9 (September, 1983), pp. L605-L607, ISSN 0021-4922

Palit, N.; and Chatterjee, P. (1998), A computer analysis of double junction solar cells with a-Si : H absorber layers, *Solar Energy Materials & Solar Cells* , Vol 53 (1998), pp. 235-245, ISSN 0927-0248.

Plá, J.; Tamasi, M.; Rizzoli, R.; Losurdo, M.; Centurioni, E.; Summonte, C. and Rubinelli, F.(2003), Optimization of ITO layers for applications in a-Si/c-Si heterojunction

solar cells , *Thin Solid Films,* Vol 425, No 1-2, (February 2003) pp. 185-192, ISSN 0040-6090.

Rahmouni, M.; Datta, A.; Chatterjee, P.; Damon-Lacoste, J.; Ballif, C. and Roca i Cabarrocas, P. (2010), Carrier transport and sensitivity issues in heterojunction with intrinsic thin layer solar cells on N-type crystalline silicon: A computer simulation study *Journal of Applied Physics,* Vol 107, No 5, (March, 2010) pp. 054521-1-14, ISSN 0021-8979.

Sakata, H.; Nakai, T.; Baba, T.; Taguchi, M.; Tsuge, S.; Uchihashi, K. and S. Kyama (2000), 20.7% highest efficiency large area (100.5 cm²) HITT™ cell, *Proceedings 28th IEEE Photovoltaic Spealist conference*, pp. 7-12, ISBN 0-7803-5772-8, Anchoorage, Alaska, 2000 September 15 -22.

Sawada, T.; Terada, N.; Tsuge, S.; Baba, T.; Takahama, T.; Wakisaka, K.; Tsuda, S. and Nakano S. (1994), High-efficiency a-Si/c-Si heterojunction solar cell, *Proceedings 1st World Conference on Photovoltaic Solar Energy Conversion*, pp.1219-1226, ISBN 0-7803-1460-3, Hawaii, USA, 1994, December 5-9.

Schmidt, M.; Korte, L.; Laades, A.; Stangl, R.; Schubert, Ch.; Angermann, H.; Conrad, E. and Maydell, K. V. (2007), Physical aspects of a-Si:H/c-Si hetero-junction solar cells , *Thin Solid Films*, Vol 515, No. 19 (July, 2007) pp. 7475-7480, ISSN 0040-6090.

Schmidt, M.; Angermann, H.; Conrad, E.; Korte, L.; Laades, A.; Maydell, K. V.; Schubert, Ch. and Strangl, R. (2006), Physical and Technological Aspects of a-Si:H/c-Si Hetero-Junction Solar Cells, *Proceedings of 4th World Conference on Photovoltaic Energy Conversion*, pp. 1433-1438, ISBN 1-4244-0017-1, Hawaii, USA, 2006, May, 7-12.

Sritharathikhun, J.; Yamamoto, H.; Miyajima, S.; Yamada, A. and Konagai, M. (2008), Optimization of Amorphous Silicon Oxide Buffer Layer for High-Efficiency p-Type Hydrogenated Microcrystalline Silicon Oxide/n-Type Crystalline Silicon Heterojunction Solar Cells, *Japanese Journal of Applied Physics*, Vol 47, No. 11, (November, 2008) pp. 8452-8455, ISSN 1347-4065.

Smole, F. and Furlan J. (1992), Effects of abrupt and graded a-Si:C:H/a-Si:H interface on internalproperties and external characteristics of p-i-n a-Si:H solar cells, *Journal of Applied Physics*, Vol 72, No. 12, (September, 1992) pp. 5964-5969, ISSN 0021-8979.

Stangl, R.; Froitzheim, A.; Elstner, L. and Fuhs, W. (2001), Amorphous/crystalline silicon heterojunction solar cells, a simulation study, *Proceedings of 17th European Photovoltaic Solar Energy Conference*, pp. 1387-1390, ISBN 3-936338-07-8, Munich, Germany, 2001, October 22-26.

Sze, S.M. (1981), *Physics of Semiconductor Devices* (2nd Edition),John Wiley & Sons, ISBN 9971-51-266-1.

Taguchi, M., Sakata, H.; Yoshihiro, Y.; Maruyama, E.; Terakawa, A.; Tanaka, M. and Kiyama, S. (2005), An approach for the higher efficiency in the HIT cells, *Proceedings of 31st IEEE Photovoltaic Specialists Conference*, pp.866 – 871, ISBN 0-7803-8707-4, Lake Buena Vista, FL, 2005, January 3-7.

Taguchi, M.; Maruyama, E. and Tanaka, M., Temperature Dependence of Amorphous/Crystalline Silicon Heterojunction Solar Cells, *Japanese Journal of Applied Physics* , Vol 47, (February, 2008), pp. 814-817, ISSN 0021-4922.

Takahama, T.; Taguchi, M.; Kuroda, S., Matsuyama, T.; Tanaka, M.; Tsuda, S.; Nakano, S. and Kuwano, Y. (1992), High efficiency single- and polycrystalline silicon solar cells

using ACJ-HIT structure,*Procedings of 11th European Photovoltaic Solar Energy Conference,* pp. 1057-1062, Montreux, Switzerland, 1992, October 12-16.

Tanaka, M.; Taguchi, M.; Matsuyama, T.; Sawada, T.; Tsuda, S.; Nakano, S.; Hanafusa, H. and Kuwano, Y. (1992), Development of New a-Si/c-Si Heterojunction Solar Cells: ACJ-HIT (Artificially Constructed Junction-Heterojunction with Intrinsic Thin-Layer), *Japanese Journal of Applied Physics*, Vol 31, (November 1992), pp. 3518-3522, ISSN 0021-4922.

Tanaka, M.; Okamoto, S.; Tsuge, S. and Kiyama, S. (2003), Development of hit solar cells with more than 21% conversion efficiency and commercialization of highest performance hit modules, *Proceedings of 3rd World Conference on Photovoltaic Energy Conversion*, Vol 1, pp. 955–958, ISBN 4-9901816-0-3, Osaka. Japan, 2003, May 11-18.

Tchakarov S., Roca i Cabarrocas P., Dutta U., Chatterjee P. and Equer B., Experimental study and modeling of reverse-bias dark currents in PIN structures using amorphous and polymorphous silicon, *Journal of Applied Physics*, Vol 94, No. 11, (December, 2003) , pp. 7317-7327. ISSN (print) 0021-8979.

van Cleef, M. W. M.; Schropp, R. E. I. and Rubinelli, F. A. (1998a), Significance of tunneling in p^+ amorphous silicon carbide *n* crystalline silicon heterojunction solar cells, *Applied Physics Letters,* Vol 73, No 18, (November, 1998), pp. 2609-2611, ISSN 0003-6951.

van Cleef, M. W. M.; Rubinelli, F. A.; Rizzoli, R.; Pinghini, R.; Schropp, R. E. I. and. van der Weg, W. F. (1998b), Amorphous Silicon Carbide/Crystalline Silicon Heterojunction Solar Cells: A Comprehensive Study of the Photocarrier Collection, *Japanese Journal Applied Physics*, Vol 37, (July, 1998), pp. 3926-3932, ISSN 1347-4065.

Veschetti, Y.; Muller, J.-C.; Damon-Lacoste, J.; Roca i Cabarrocas, P.; Gudovskikh, A. S.; Kleider, J.-P.; Ribeyron, P.-J. and Rolland, E. (2006), Optimisation of amorphous and polymorphous thin silicon layers for the formation of the front-side of heterojunction solar cells on p-type crystalline silicon substrates, *Thin Solid Films*, Vol 511-512, (July, 2006), pp. 543-547, ISSN 0040-6090.

von der Linden M. B., Schropp R. E. I., van Sark W. G. J. H. M., Zeman M., Tao G. and Metselaar J. W., The influence of TCO texture on the spectral response of a-Si:H solar cells, *Proceedings of 11th European Photovoltaic Solar Energy Conference*, pp. 647 Montreux, Switzerland, 1992, October 12-16.

Wang, Q.; Page, M.; Yan, Y. and Wang, T. (2005), High-throughput approaches to optimization of crystal silicon surface passivation and heterojunction solar cells, *Proceedings of the 31st IEEE Photovoltaic Specialists Conference*, pp.1233-1236, ISBN 0-7803-8707-4, Orlando, FL, USA, 2005, January 3-7.

Wang, Q.; Page, M.R.; Iwaniczko, E.; Xu, Y.Q.; Roybal, L.; Bauer, R.; To, B.; Yuan, H.C.; Duda, A. and Yan, Y.F., Crystal silicon heterojunction solar cells by hot-wire CVD, *Proceedings of the 33rd IEEE Photovoltaic Specialists Conference*,pp 1-5, ISBN: 978-1-4244-1640-0, San Diego, CA, USA, 2008, May 11-16.

Wang, Q.; Page, M. R.; Iwaniczko, E.; Xu, Y.; Roybal, L.; Bauer, R.; To, B.; Yuan, H.-C.; Duda, A.; Hasoon, F.; Yan, Y. F.; Levi, D.; Meier, D.; Branz Howard, M. and Wang, T. H. (2010), Efficient heterojunction solar cells on *p*-type crystal silicon wafers, *Applied Physics Letters,* Vol 96, No. 1, (January, 2010), pp. 013507-1-3, ISSN 0003-6951.

Zeman, M.; van Swaaij, R. A. C. M. M.; Metselaar, J. W. and Schropp, R. E. I. (2000), Optical modeling of *a*-Si:H solar cells with rough interfaces: Effect of back contact and

interface roughness, *Journal Applied Physics* , Vol 88, No. 11 (December, 2000) pp. 6436-6443, ISSN 0021-8979.

News release by SANYO on 22nd May, 2009, SANYO Develops HIT Solar Cells with World's Highest Energy Conversion Efficiency of 23.0%.
< http://panasonic.net/sanyo/news/2009/05/22-1.html>.

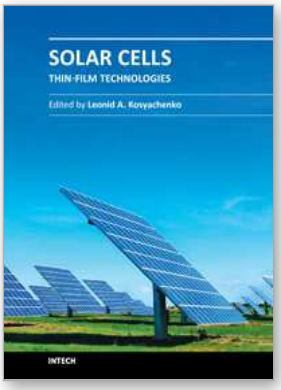

Solar Cells - Thin-Film Technologies

Edited by Prof. Leonid A. Kosyachenko

ISBN 978-953-307-570-9
Hard cover, 456 pages
Publisher InTech
Published online 02, November, 2011
Published in print edition November, 2011

The first book of this four-volume edition is dedicated to one of the most promising areas of photovoltaics, which has already reached a large-scale production of the second-generation thin-film solar modules and has resulted in building the powerful solar plants in several countries around the world. Thin-film technologies using direct-gap semiconductors such as CIGS and CdTe offer the lowest manufacturing costs and are becoming more prevalent in the industry allowing to improve manufacturability of the production at significantly larger scales than for wafer or ribbon Si modules. It is only a matter of time before thin films like CIGS and CdTe will replace wafer-based silicon solar cells as the dominant photovoltaic technology. Photoelectric efficiency of thin-film solar modules is still far from the theoretical limit. The scientific and technological problems of increasing this key parameter of the solar cell are discussed in several chapters of this volume.

InTech Europe
University Campus STeP Ri
Slavka Krautzeka 83/A
51000 Rijeka, Croatia
Phone: +385 (51) 770 447
Fax: +385 (51) 686 166
www.intechopen.com

InTech China
Unit 405, Office Block, Hotel Equatorial Shanghai
No.65, Yan An Road (West), Shanghai, 200040, China
中国上海市延安西路65号上海国际贵都大饭店办公楼405单元
Phone: +86-21-62489820
Fax: +86-21-62489821